Investigating the Surface Properties of Polyurethane Based Anti-Graffiti Coatings Against UV Exposure

A. Mohammad Rabea,[1] S. M. Mirabedini,[2] M. Mohseni[1]

[1]*Department of Polymer Engineering and Color Technology, Amirkabir University of Technology, Tehran, Iran*
[2]*Iran Polymer & Petrochemical Institute, Tehran, Iran*

Received 14 November 2010; accepted 23 July 2011
DOI 10.1002/app.35344
Published online 3 November 2011 in Wiley Online Library (wileyonlinelibrary.com).

ABSTRACT: A permanent anti-graffiti coating based on a polyurethane resin was prepared by incorporating different levels of an OH-functional silicone modified polyacrylate additive. Static contact angle measurements and dynamic mechanical thermal analysis (DMTA) were employed to evaluate surface free energy and mechanical properties of the coating specimens, respectively. Effect of ageing condition on the graffiti properties of the coating samples was evaluated utilizing an accelerated weathering test. Color changes, surface morphology, and variations in the mechanical properties were also examined prior to and after being exposed to UV irradiation for 864 h in a QUV chamber. Results showed that surface free energy of the samples decreased with replacement of polyol with additive up to 5 mol %. A Scanning electron microscope equipped with energy dispersive X-ray detector revealed that for the samples containing more than 5 mol % additive, there was an enrichment of silicone at the interface of films and air. At long exposure times and higher concentrations of additive, depreciation of graffiti properties was seen. DMTA and attenuated total reflectance-fourier transform infra-red studies before and after ageing showed that the silicone additive tended to degrade while it could cause an increase in crosslinking density. Water contact angles and atomic force microscopy images after ageing revealed that the cause of the depletion in anti-graffiti properties was attributed to the deterioration of the silicone additive. © 2011 Wiley Periodicals, Inc. J Appl Polym Sci 124: 3082–3091, 2012

Key words: polyurethanes; silicones; surface modification; degradation; ageing

INTRODUCTION

Developing coatings with anti-graffiti properties has been taken into account as an active field of research for many years in the coating industries. The usual strategy for obtaining such coatings is based on the surface free energy modulation utilizing flouro, perfluoro, or silicone components in the formulation,[1] to prevent the graffiti wetting the surface. The resulting coatings will then be cleaned more easily, so the life time of coatings will be longer. In addition, the use of aggressive cleaning agents and tedious removing methods will be reduced extensively.[2]

Polysiloxanes are well known for their appropriate properties such as, hydrophobicity, thermal stability, and biological resistance.[3] However, inferior optical resistance was reported as one of the disadvantages of siloxane products.[4] Gommans studied the chemistry of polysiloxanes with respect to the environmental and durability aspects of these materials.[3] The polysiloxane modified polyurethanes (Si-PU) are able to show both properties of polysiloxanes and polyurethanes. These properties included good thermal stability, freeze resistance, insulativity, flexibility, cohesiveness, wear resistance, surface property, and hydrophobicity.[5–14] Feng et al.[15] investigated the surface properties of polyurethanes modified by polysiloxane. No evaluation, however, on the anti-graffiti properties and weatherability of such coatings has been reported so far.

In our previous work,[16] a series of silicone containing PUs were prepared using an OH-functional silicone modified polyacrylate additive. The effects of this additive on the surface chemistry, mechanical, and anti-graffiti properties were investigated. In this study, we aim at revealing the mechanism of operation of polysiloxane additive and the longevity of the resultant coatings against an accelerated weathering test. Mechanical, chemical, and surface properties of the aged samples are then evaluated.

EXPERIMENTAL

Materials and methods

BYK-SILCLEAN 3700 (a solution of 25 wt % OH-functional silicone modified polyacrylate in methoxypropylacetate), was obtained from BYK

Correspondence to: M. Mohseni (mohseni@aut.ac.ir).
Contract grant sponsors: Department of Polymer Engineering and Color Technology, Amirkabir University of Technology, Tehran.

TABLE I
Formulation of Various Samples for Preparation of Anti-Graffiti Coatings

Sample coding[a]	BYK-SILCLEAN 3700 (wt %)	Uracrone CY433 (wt %)	Desmodure N75 (wt %)
PU0	–	67.3	32.7
PU2	3.8	64.3	31.9
PU5	9.3	60.0	30.7
PU10	17.6	53.5	28.9
PU15	25.0	47.7	27.3
PU100	86.0	–	14.0

[a] The number shows the mol % of polyol, which is substituted with the additive.

(Germany) Altana group and used as received. The acrylic polyol, Uracrone CY433 (60 wt % solution in xylene/butyl acetate mixture) was provided by DSM (Netherlands). An aliphatic polyisocyanate hardner based on hexamethylene diisocyanate (HDI) (Desmodure N75), supplied by Bayer Co. (Germany), was used as curing agent. It was a solution of 75 wt % in xylene/methoxy propyl acetate mixture. No catalyst was used. The molar ratio of -OH : -NCO was 1 : 1.2. All other chemicals were of analytical grade and used without further purification.

For preparation of coatings,[16] various amounts of acrylic polyol were substituted with the additive within the range of 2, 5, 10, and 15 mol %, followed by mixing for 15 min under a moderate shear rate. Once the proper dispersion was achieved, isocyanate curing agent was added to the solution and further stirred for 15 min. Two coating samples; polyurethane without anti-graffiti additive (PU0) and the one in which the additive was used instead of the whole acrylic polyol (PU100) were also prepared as the reference samples. Various formulations of prepared anti-graffiti coatings are listed in Table I. To show the effect of additive hydroxyl groups on the polyurethane curing process, the additive was partially replaced with the polyol.

Prepared coating samples were then applied on the degreased glass substrates using a film applicator (BYK-Gardner). The samples were then left for at least 1 week in ambient temperature to reach the maximum possible curing state and acquire the highest physical and mechanical properties. The films were 35 ± 5 μm thick.

Surface free energy calculations

Wettability of the specimens was evaluated by static contact angle measurements using a "KRUSS" G2/G40 system. The procedure used to measure the contact angle was based on ASTM D 724 standard. Probe test liquids (analytical grade), with different values of surface tension (γ_l), were utilized to determine surface energy of the coating specimens. For reliable determination of the surface energy, a relatively wide range of liquids from very polar to nonpolar were used as shown in Table II. Three droplets of each liquid were tested on the surface of coating specimens to ensure the statistical validity of the results. The measurement was completed after about 30 s.

Several methods are available for calculation of the surface free energy of a solid,[17] the particular method adopted depends on the surface to be examined and the selected test liquids. In this study, Wu and Nancollas[18] [eqs. (1) and (3)] and Owens–Wendt[19] models [eqs. (2) and (3)] were employed to calculate the surface free energy of the coating samples, respectively.

$$\gamma_{lv}(1+\cos\theta) = 4\left(\frac{\gamma_{sv}^{p}\gamma_{lv}^{p}}{\gamma_{sv}^{p}+\gamma_{lv}^{p}} + \frac{\gamma_{sv}^{d}\gamma_{lv}^{d}}{\gamma_{sv}^{d}+\gamma_{lv}^{d}}\right) \quad (1)$$

$$\gamma_{lv}(1+\cos\theta) = 2\sqrt{\gamma_{sv}^{p}\gamma_{lv}^{p}} + 2\sqrt{\gamma_{sv}^{d}\gamma_{lv}^{d}} \quad (2)$$

$$\gamma_{sv} = \gamma_{sv}^{p} + \gamma_{sv}^{d} \quad (3)$$

where, γ_{lv} is the liquid–vapor interfacial tension and θ represents the Young's contact angle. γ_{sv}^{p} and γ_{sv}^{d} are the polar and disperse components of the surface free energy of solid, respectively. γ_{lv}^{p} and γ_{lv}^{d} are the polar and disperse components of surface tension of the probe liquid. γ_{sv} is the total surface free energy of the solid.

Morphological studies

An Oxford IncaPenta FETX 3 SEM/energy dispersive X-ray detector (EDX) was used to examine the morphology of the coating samples. To examine the cross-section, samples were broken in liquid nitrogen. Then specimens were sputter coated with a very thin layer of gold. Silicone element was mapped using an appropriate detector.

Ageing property

For evaluation of the ageing property of the coatings, a black permanent marker (STAEDTLER) was used. An area of 4 cm × 4 cm of the coated glass substrate was marked. Black marked samples and free standing film specimens were then placed in a

TABLE II
Surface Free Energy Values of Probe Liquids

	Surface tension (mN/m)		
Probe liquids	γ_{1v}^{d}	γ_{1v}^{p}	γ_{1v}
Water	21.8	51.0	72.8
Diodomethene	50.8	0.0	50.8
Benzyl alcohol	28.6	11.4	40.0

QUV chamber for about 864 h. Accelerated weathering test was carried out according to the ASTM G 154, (Fluorescent UV-Condensation Type (Model QUV/Spray, Q-Panel Co.). According to the procedure, the specimens were alternately exposed to repeated cycles of UVA radiation (340 nm, energy of 0.89 W/m^2) at 60°C for 8 h, followed by 4 h in humid condition (100 RH%) at 50°C. At each 144 h of exposure, black marked coatings were cleaned by a dry paper tissue and color attributes (L a^*b^*) and total color change (ΔE) were measured. Utilizing a Miniscan XE Plus (Hunter lab Co.) colorimeter in 45° angle, ΔE of the coating samples as a function of UV irradiation was calculated using CIE 1976 formula [eq. (4)], where ΔL, Δa^*, and Δb^* are differences in lightness (L value), red/green (a^* value), and blue/yellow (b^* value) color coordinates before and after exposure.[20]

The cleaned samples were again stained by marker and then exposed to UVA for further 144 h. This cycle was repeated for six times, and ΔE of coating samples at the end of each cycle was recorded as an indication of the extent of graffiti removal of aged samples.

$$\Delta E_{ab} = \sqrt{(\Delta L)^2 + (\Delta a^*)^2 + (\Delta b^*)^2} \quad (4)$$

Dynamic mechanical thermal analysis

A dynamic mechanical thermal analysis (DMTA) analysis was carried out with a DMA-TRITON Model Tritec 2000 instrument at temperature range between 30 and 130°C, at frequency of 1 Hz. The mode of the analysis was tension and heating rate was 5 °C/min (according to ASTM E 1640).

Attenuated total reflectance analysis

Attenuated total reflectance (ATR)-FTIR spectra were recorded and analyzed using an FTIR spectrometer model Equinox X-55, collecting 35 scans in the 400–4000 cm^{-1} range with 4 cm^{-1} resolution, in the transmission mode before and after 864 h exposure in QUV chamber.

Atomic force microscopy

Atomic force microscopy (AFM, Dual scope/Rasterscope C26, DME) was used to examine the effect of accelerated weathering condition on the coatings surface topography of various coating samples. Free standing film samples were removed from QUV chamber after 864 h exposure and then 100 mm^2 (45 μm thickness) specimen was cut for AFM studies. The AFM experiments were conducted at noncontact mode with a rectangular cantilever and a conical tip, respectively. The length, width, and thickness of the cantilever were 460, 50, and 2 microns. Also the force and distance between the tip of the cantilever and surface of the samples were around 0.15 nN and 10–100 Å, respectively.

TABLE III
Contact Angles (θ) of Water, Diiodomethene, and Benzyl Alcohol on the Coating's Films

Sample coding	Water	Diodomethene	Benzyl alcohol
PU0	81.1	47.7	[a]
PU2	100.9	72	51.4
PU5	103.7	75.7	63.2
PU10	103.7	78.4	64.3
PU15	104.1	76.7	63.6
PU100	106.6	77.3	71.2

[a] Benzyl alcohol could completely wet PU0.

RESULTS AND DISCUSSION

Surface studies

Contact angle measurements of various probe liquids on the coating specimens are listed in Table III. As it can be seen, with only 2 mol % of the additive, water contact angle was increased considerably. However, with further increasing level of additive, the contact angles of various probe liquids were not increased significantly. There is a negligible change in the contact angle for samples containing 5 mol % and higher additive levels. Since the contact angles exceeded 90°, the samples containing 2 mol % and higher would be considered hydrophobic.

Benzyl alcohol could spread completely on the PU0 sample; however, it behaved differently for PU2 sample, showing that the surface energy of the PU0 sample is higher than that of the benzyl alcohol (40 mN/m).

Based on the contact angle measurements, the corresponding free energy of the surface was calculated by means of the Owen and Wendt[19] and Wu and Nancollas[18] methods, and results were plotted against additive concentration as shown in Figure 1.

As it is evident, by increasing the additive content up to 5 wt %, the surface free energy has decreased. This can be attributed to migration of siliconated additive to the surface of films. However, further increase of additive, leads to a relatively constant surface free energy, perhaps due to the saturation of surface with additive chains. Disperse and polar components have decreased by increasing additive concentration. However, the polar component has not varied considerably for samples containing 5 mol % and higher. This leads to a poor interaction of the coating with polar molecules such as water, indicating an improved hydrophobicity.

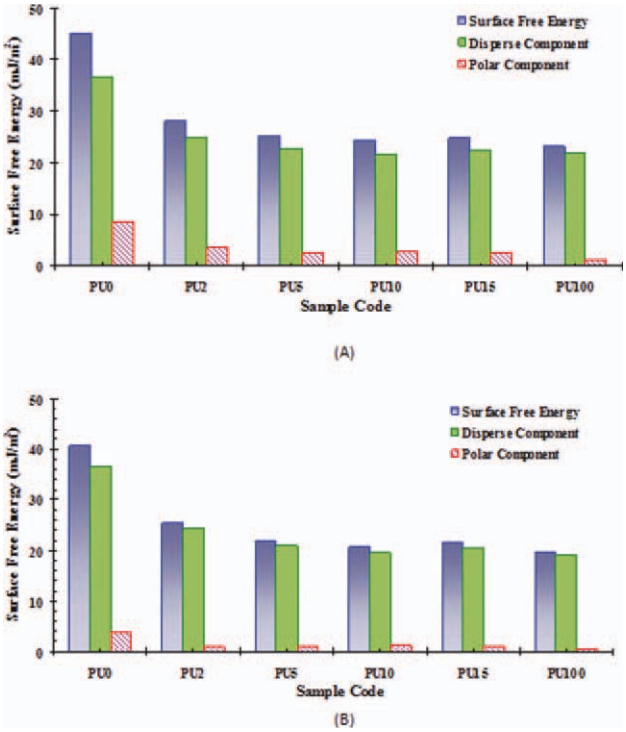

Figure 1 Surface free energy of the coating samples obtained from: (A) Wu method; (B) Owens–Wendt method. [Color figure can be viewed in the online issue, which is available at wileyonlinelibrary.com.]

It can be discussed that, as the surface free energy of the PU0 is more than that of benzyl alcohol, the surface free energies calculated by the Wu model seem more reliable. The reason is that the surface free energy of PU0 by Wu model is 45.13 mJ/m^2. This is greater than the surface tension of benzyl alcohol. That is why benzyl alcohol wets PU0 completely. However, the surface free energy of PU0 based on Owens–Wendt model (40.55 mJ/m^2) is similar to that of benzyl alcohol. It means that by Owens–Wendt model, this liquid could slightly wet PU0. Also, for PU2, as its surface energy (28.11 mJ/m^2) is lower than that of benzyl alcohol, an increase in contact angle seems plausible.

Further analysis was performed with an SEM equipped with EDX. Figure 2 depicts the micrographs of samples PU0, PU5, and PU10 taken from surfaces and cross-section of films, respectively.

These micrographs show crack-free and smooth surfaces. There is not much difference between micrographs of samples PU5 and PU10 in Figure 2. Also, in this figure, SEM cross-section images for PU0 and PU5 are almost similar. However, there can be seen that cross-sectional SEM micrograph of sample PU10 varies slightly. Further analysis was performed using EDX technique by which silicone was mapped. Figure 3 shows the results of such an analysis.

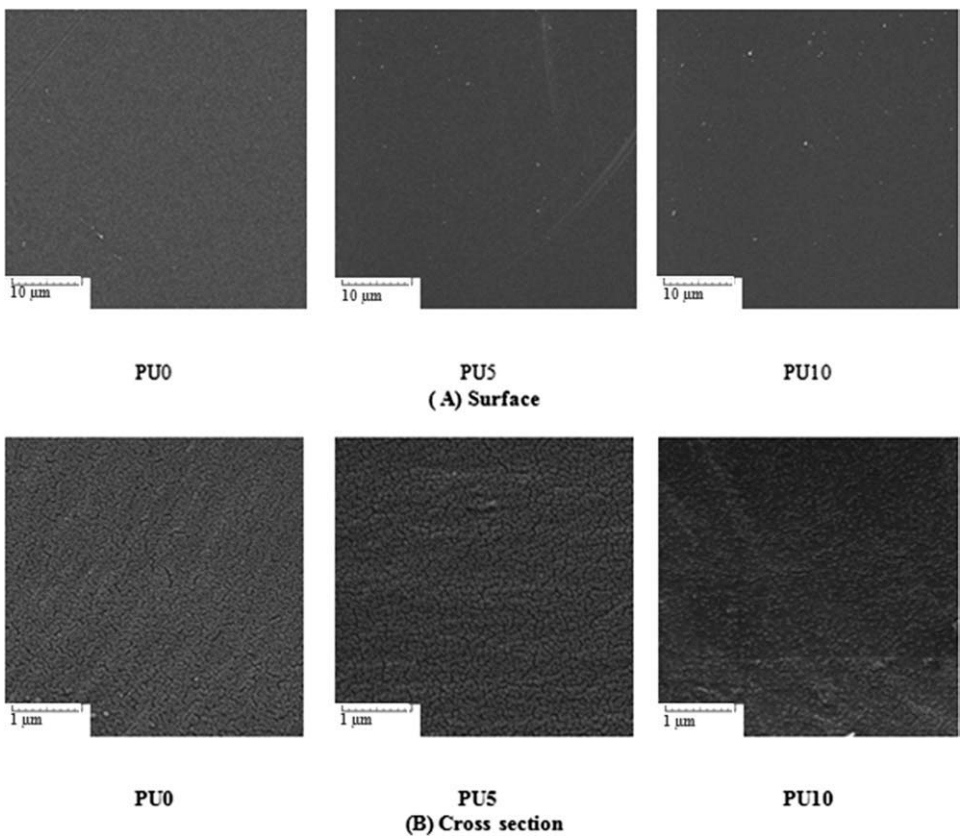

Figure 2 SEM images of different specimens at (A) surface and (B) cross-section.

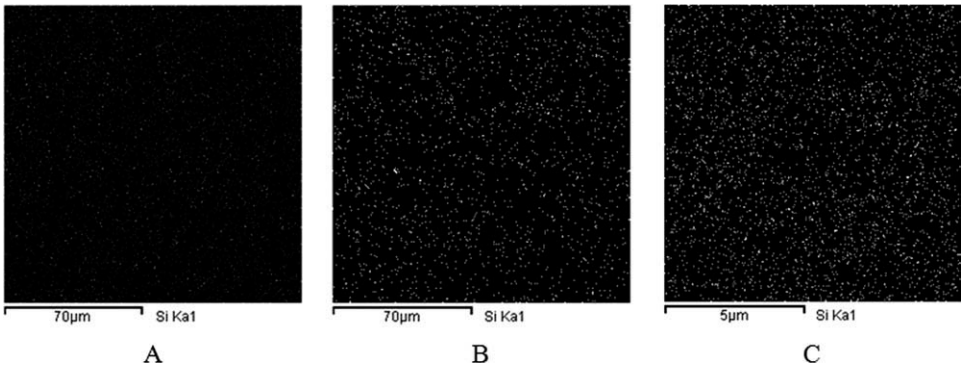

Figure 3 Silicone mapping of (A) surface of PU5; (B) surface of PU10, and (C) cross-section of PU10.

The existence of silicone at the surface of PU5 and PU10 may explain surface tension data. EDX analysis could not reveal the presence of silicon inside the film. However, at concentrations greater than 5 mol %, silicon is clearly mapped. It may be concluded that for samples containing 5 mol % of additive, there is an enrichment of silicon at the surface. These results are in agreement with the data given by surface energies calculations. In fact, the constant value of surface energy for samples containing 5 mol % of additive can be justified with these observations.

Ageing properties

To numerically compare the coatings appearance upon exposure to graffiti marking, the color attributes, L, a^*, and b^*, (numbers are the average of three different measurements) for each ageing cycle were recorded as listed in Table IV. As it can be seen, the incorporation of the additive does not have any effect on the color data of films. In other words, the color attributes are the same before execution of the first cycle. However, after each cycle, there is a reduction in color attributes. As such, samples become more green and blue in color. Moreover, the lightness changes noticeably by inclusion of additive. After the second cycle, the lightness of PU100 changes to 56.7, which is even smaller than that of PU0 (64.92). This is one of the drawbacks of anti-graffiti coatings based on silicone additives, as also discussed by Tarnowski et al.[4] and Graiver et al.[21]

TABLE IV
Color Data, L^*, a^*, b^*, and ΔE for Different Samples at Each Cycle

		Cycle						
Color data	Sample	0 (Without graffiti)	1	2	3	4	5	6
L	PU0	88.43	65.12	64.92	62.8	62.07	61.84	58.57
	PU2	88.37	69.21	66.3	64.92	63.83	62.27	62.14
	PU5	88.43	77.18	71.2	65.8	64.96	61.91	61.01
	PU10	88.54	78.61	72.81	63.39	61.74	59.89	59.72
	PU15	88.63	77.54	64.8	64.98	63.41	59.04	56.46
	PU100	88.49	77.43	56.7	54.69	52.67	51.01	48.34
a^*	PU0	−2.73	−5.42	−5.29	−5.46	−5.42	−5.27	−5.47
	PU2	−2.71	−5.04	−5.18	−5.12	−5.25	−5.43	−5.40
	PU5	−2.67	−4.52	−5	−5.89	−5.78	−6.04	−6.08
	PU10	−2.73	−3.22	−3.81	−4.91	−5.06	−5.08	−4.96
	PU15	−2.66	−3.24	−4.61	−4.52	−4.62	−4.94	−5.05
	PU100	−2.55	−3.04	−5.04	−4.57	−4.9	−4.69	−4.83
b^*	PU0	1.48	−6.98	−7	−7.4	−7.45	−7.46	−8.19
	PU2	1.24	−5.31	−5.82	−6.28	−6.61	−6.87	−6.90
	PU5	1.25	−2.64	−4.11	−6.02	−6.06	−6.9	−7.11
	PU10	1.32	−2.16	−3.85	−6.51	−6.94	−7.3	−7.33
	PU15	1.25	−2.4	−5.9	−5.93	−6.4	−7.41	−8.02
	PU100	1.24	−2.59	−8.32	−8.78	−9.24	−9.43	−9.93
ΔE	PU0	–	24.94	25.12	27.26	27.96	28.17	31.5
	PU2	–	20.38	23.3	24.74	25.89	27.47	27.76
	PU5	–	12.05	18.2	23.99	24.78	27.95	28.87
	PU10	–	10.53	16.59	26.43	28.14	30.01	30.17
	PU15	–	11.69	24.96	24.79	26.43	30.92	33.56
	PU100	–	11.71	33.29	35.31	37.4	39.03	41.74

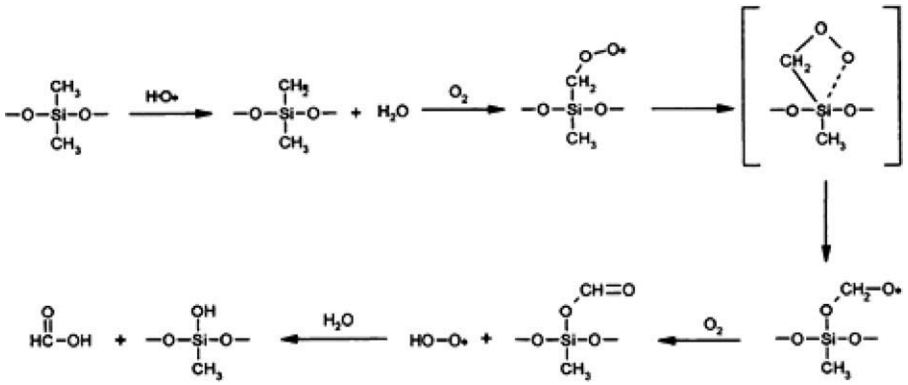

Scheme 1 Chemical path for the conversion of methylene pendant groups of silicone chains to hydroxyl groups.[21]

Linear silicone polymers and cyclosiloxanes can be readily degraded in the environment by natural processes. This is perhaps because the methylene pendant groups of silicone chains change to hydroxyl groups as discussed by Gravier et al. as depicted in Scheme 1.[21] As can be seen, after the first cycle PU2 has the lowest lightness among other samples containing additive.

Color difference, ΔE, before and after the graffiti removal for each cycle is shown in Figure 4. It can be seen that color difference increases by increasing the number of cycles. PU100 shows the greatest ΔE increase while that of PU0 is the lowest. Interestingly, PU0 shows the highest ΔE after the first cycle, but it almost retains its ΔE during further cycles. It is obvious that after the first cycle, the color difference of PU2 is similar to that of PU0. In addition, for other samples containing more than 5 mol % additive color difference has not changed by increasing the additive concentration.

As discussed in our previous work,[16] depreciation of anti-graffiti properties of samples could be related to the decrease in crosslinking density or increase in surface free energy of samples. To this end, mechanical properties and surface functional groups were studied by DMTA and ATR-FTIR spectroscopy, respectively.

The results of DMTA analysis for PU0, PU5, and PU100 before and after 864 h exposure in QUV (at the end of sixth cycle) are shown in Figure 5. T_g of samples before and after ageing are listed in Table V.

According to DMTA results, for PU0 due to the formation of polar bonds between chains, there is an

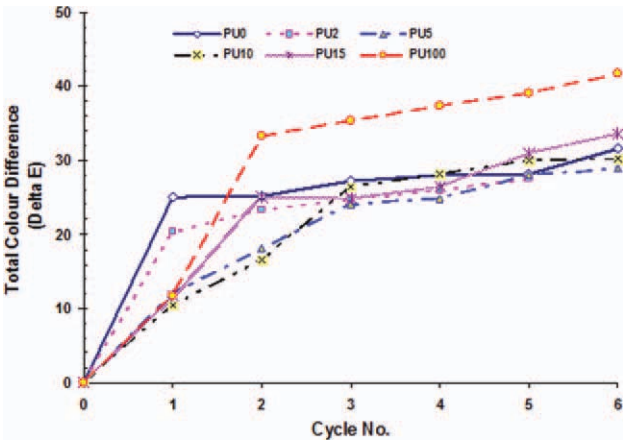

Figure 4 Color difference, ΔE, before and after the graffiti removal for each cycle. [Color figure can be viewed in the online issue, which is available at wileyonlinelibrary.com.]

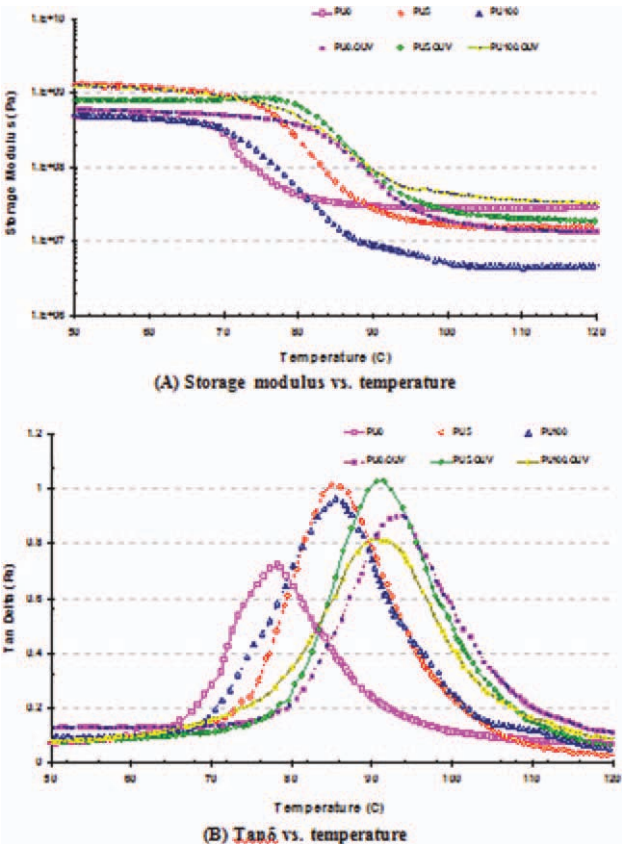

Figure 5 DMTA results obtained for different coating specimens before and after 864 h exposure in QUV chamber. [Color figure can be viewed in the online issue, which is available at wileyonlinelibrary.com.]

TABLE V
Variations of Area Under ATR-FTIR Peaks, Water Contact Angles, and Glass Transition Temperatures of Samples Before (a) and After (b) 864 h Exposure to QUV

			Area under ATR-FTIR peaks						
	T_g		781–837 cm^{-1} (Si—OH)		1000–1045 cm^{-1} (Si—O—Si)		Water contact angles (%)		
Sample coding	(a)	(b)	(a)	(b)	(a)	(b)	(a)	(b)	Reduction in contact angle %
PU0	78.2	93.9	0.00	0.00	0.00	0.00	81.1	79.9	1.48
PU5	84.9	91.5	0.16	0.39	0.59	1.48	103.7	81.7	21.22
PU100	85.5	90.9	0.43	16.3	1.44	4.1	106.6	77.1	27.67

increase in storage modulus in glassy region. However, in rubbery region, because of the reduction in the number of these polar bonds, the mechanical properties become worse. Also, an increase in the area under the tan δ versus temperature for PU0 after ageing (PU0-QUV) is another evidence for the presence of these physical bonds. For PU5, as there is not any significant change in storage modulus in rubbery region before and after UV exposure, there is likely that siloxane bonds (Si—O—Si) between hydroxyl groups have formed.[21] Accordingly, these may have increased the T_g and the mechanical properties in the rubbery region. Finally, for PU100, because of high concentration of hydroxyl groups and high probability of formation of siloxane bonds, there is a dramatic improvement in mechanical properties in rubbery region. Also, because of increase in crosslinking density by formation of these siloxane bonds, T_g has increased and the area under the tan δ versus temperature has decreased. This seems to be the reason for formation of chemical bonds and lower damping behavior.

These results are in agreement with the work of Kim and Urban,[22] who discussed the mechanism of degradation of polyurethane. They reported that in polyurethane coatings during QUV condition, degradation of polymer chains occurred, leading to decline in crosslinking density and reduction in mechanical properties. Polar groups which are produced by degradation can make polar–polar interactions and increase the mechanical properties in glassy region. These lead to increase in T_g and the area under the tan δ peaks, indicating a damping phenomenon. In rubbery region, however, these polar bonds start to break and reduce the mechanical properties.

Interestingly, in PU100 despite an increase in crosslinking density, it showed the worst result during ageing. It may be because of the formation of polar groups during degradation and increasing of surface free energy.

To confirm the results of DMTA, ATR-FTIR analysis was done for different samples before and after ageing. Normalized ATR-FTIR spectra for PU0, PU5, and PU100, with respect to the C—H vibration bond in PU0, before and after 864 h in QUV condition have been shown in Figure 6.

There can be seen that the difference between PU0 and PU5 before and after the ageing is negligible. But for PU100, there is seen a more noticeable difference. So, it shows that more degradation may have been occurred for this sample. The mechanism of degradation of polyurethane in QUV condition was also discussed by Jalili and Moradian[23] The area under the peaks for different functional groups has been deduced from Figure 6 as shown in Table V.

As can be seen in Table V in PU0 sample, the area under the peak at 781–837 cm^{-1} corresponding to Si—OH group is zero, as expected. However, for PU5 it changes from 0.16 (before ageing) to 0.39 (after ageing). Also, there is a profound change for PU100 from 0.43 (before ageing) to 16.3 (after ageing). These observations well agree with the findings of Graiver et al.,[21] who showed that linear silicone

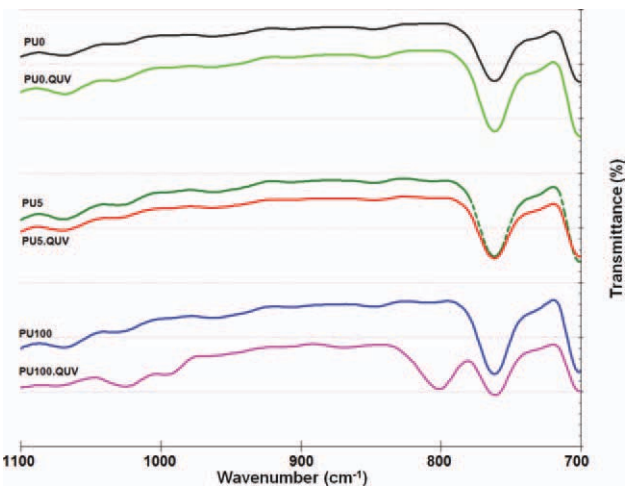

Figure 6 Normalized ATR spectra for PU0, PU5, and PU100, before and after 864 h exposure in QUV chamber. [Color figure can be viewed in the online issue, which is available at wileyonlinelibrary.com.]

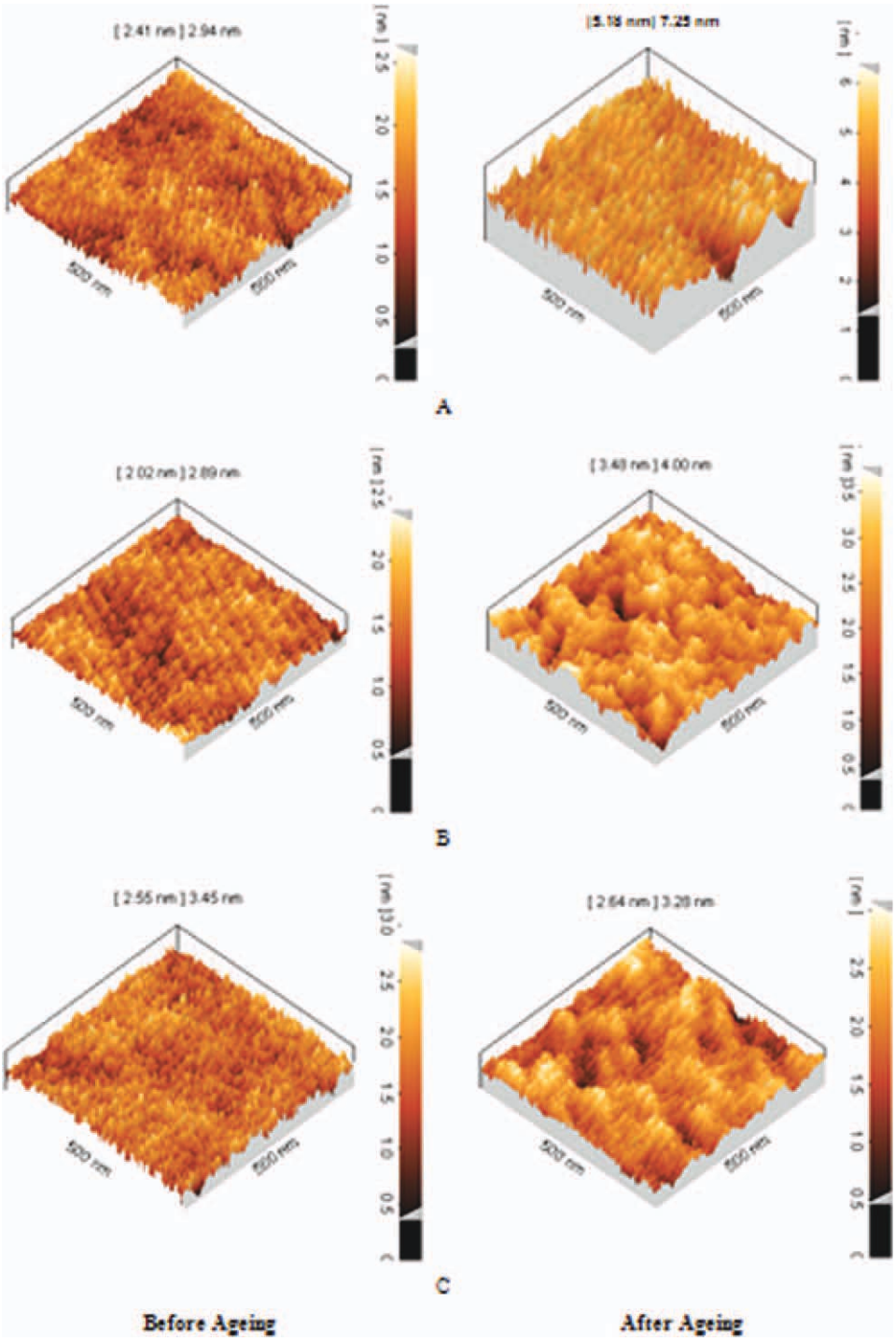

Figure 7 AFM images of (A) PU0; (B) PU5; (C) PU100 before and after 864 h exposure in QUV chamber. [Color figure can be viewed in the online issue, which is available at wileyonlinelibrary.com.]

polymers could be degraded by natural processes. This, as mentioned above, was attributed to the fact that methylene pendant groups of silicone chains changed to hydroxyl groups. Also, the area under the peak at 1000–1045 cm^{-1} attributed to Si—O—Si, for PU5 changes from 0.59 (before ageing) to 1.48 (after ageing). For PU100 this occurs from 1.44 (before ageing) to 4.1. Therefore, the increase in crosslinking density of PU100 in rubbery region can be ascribed to the formation of siloxane bonds.

The fact that the anti-graffiti behavior of PU100 changed noticeably during QUV cycles, could be explained to the decreased crosslinking density or increased surface free energy. DMTA results showed that crosslinking density of this sample did not decrease. However, as can be seen in Table V, the

water contact angle for this sample has declined noticeably after ageing. This means that this sample has become more hydrophilic.

Table V shows that there is only a little decrease in water contact angle for PU0 after ageing. However, those of PU5 and PU100 are more notable. It reveals that after ageing, surface free energy of samples containing additive have increased, because of the formation of hydroxyl groups. This phenomenon corresponds to inferior anti-graffiti properties upon ageing.

To further study the above observations, surface topography of samples were investigated using AFM. Figure 7 shows AFM images of PU0, PU5, and PU100 samples before and after ageing. AFM images show that samples containing silicone additive have been etched under QUV condition. There are no obvious severe etched areas in PU0 image. As can be seen from Figure 7 PU0 has been roughened to a more extent after ageing (from 2.41 nm to 5.16 nm). However, the distribution of roughnesses and the existence of pits and valleys are completely homogeneous. While AFM images of samples PU5 and PU100 show heterogeneously scattered rough topography, which are indicative of an etched surface. This means that the presence of additive has resulted in degradation.

According to Wenzel model [eq. (5)],[24] the relation between the contact angles of a rough surface to that of a smooth one is as follows:

$$\cos\theta_i = i * \cos\theta \tag{5}$$

where, θ_i is the contact angle of liquid on a rough surface, θ is the contact angle of liquid on the smooth surface with the same chemical composition and "*i*" is the roughness factor. Moreover, based on the Wenzel equation parameter "ii" is also related to the interfacial surface area. Accordingly, it seems that the interfacial surface area of PU5 and PU100 after ageing has comparatively increased. This may possibly explain the greater reduction in contact angles of PU5 and PU100 after ageing, showing that the higher hydrophilic nature of these samples upon UV exposure. This is in well agreement with the results of area under the FTIR peaks corresponding to Si—OH groups as shown in Table V. Therefore, the quantities of contact angles of water on the surfaces of PU5 and PU100 reveal the discernable change in surface chemistry of these samples after ageing. This may be the plausible reason for the lowered water contact angles reported in Table V.

This much-quoted equation immediately suggests that if $\theta < 90^\circ$ then $\theta_i < \theta$, but if $\theta > 90^\circ$ then $\theta_i > \theta$. In other words, as the roughness factors of the additive containing samples are lower than 90° upon ageing, the higher the *i*, the smaller is the equilibrium water contact angle and the greater is the chance of surface to be wetted. This enhanced wettability of the roughened surface of PU5 and PU100 after being exposed to UV radiation is a real concern for these types of silicon containing coatings that leads to inferior anti-graffiti properties in spite of having a proper behavior before exposure to environment. Attempts are being made in our lab to replace the silicon type additives with fluorinated ones to avoid such degradations. Also, we are currently working on improving the UV resistance of these coatings using nanosized metal oxide particles such as nano silica. The results of decreased surface ablation under UV exposure have been promising. The positive point obtained with the fluorinated additive was a profound increase in water contact angle to as high as 135°, maintaining the UV resistance of films similar to that of polyurethane without additive.

In the nano silica loaded films, however, the contact angles obtained were not significantly changed. But, the color change upon UV irradiation markedly declined almost 50%, probably due to the UV absorbing ability of nano silica. However, the use of these new approaches has not been without difficulty. For example, the reduced surface tension of the polyurethane clear coat in the liquid state makes it slightly retract when applied, and needs special attention to balance the leveling agent content of the formulation. In silica loaded films, the dispersion of nano particles showed to be a real concern. The results of these attempts will be reported in future works.

CONCLUSIONS

The purpose of this article was to prepare polyurethane coatings with anti-graffiti properties. A silicone acrylic additive was included in the formulation to reach such a behavior. It was observed that surface free energy of the samples decreased with replacement of the polyol with the additive up to 5 mol %, after which a constant trend was observed, presumably due to the migration of the additive to the surface of films. This resulted in an effective anti-graffiti characteristic. However, ageing of the samples under UV condition revealed that the inclusion of additive could affect the films negatively. By increasing in number of the UV exposure cycles and additive concentration, samples showed inferior results because of degradation of the additive. Mechanical and surface evaluation of aged samples also revealed that the decrease in anti-graffiti properties during UV cycles was most likely related to degradation of silicone additive. Therefore, it can be predicted that by improving the UV resistance of films against weathering, the anti-graffiti behavior will not be influenced. This could be accomplished

by inclusion of UV absorbing ingredients in the formulation, such as silica nano particles, or alternatively by using fluorinated containing additives.

References

1. Wu, X.; Rosen, R. P. JCT Coat Technol 2008, 5, 66.
2. Scheerder, J.; Visscher, N.; Nabuurs, T.; Overbeek, A. JCT Res 2005, 2, 617.
3. Gommans, L. Corrosion Prevent 2000, Paper 072, 1.
4. Tarnowski, A.; Zhang, X.; McNamara, C.; Martin, S. T.; Mitchell, R. J ACCR 2007, 32, 3.
5. Liao, S. K.; Jang, S. C.; Lin, M. F. J Polym Res 2005, 12, 103.
6. Stanciu, A.; Bulacovschi, V.; Oprea, S.; Vlad, S. Polym Degrad Stab 2001, 72, 551.
7. Vlad, S.; Vlad, A.; Oprea, S. Eur Polym Mater 2002, 38, 829.
8. Zhu, Q.; Feng, S.; Zhang, C. J Appl Polym Sci 2003, 90, 310.
9. Dolmaire, N.; Me'chin, F.; Espuche, E.; Pascault, J. P. J Polym Sci Part B: Polym Phys 2006, 44, 48.
10. Kayaman-Apohan, N.; Amanoel, A.; Arsu, N.; Gungor, A. Prog Org Coat 2004, 49, 23.
11. Bremner, T.; Hill, D. J. T.; Killeen, M. I.; O'Donnell, J. H.; Pomery, P. J.; John, D. S.; Whittaker, A. K. J Appl Polym Sci 1997, 65, 939.
12. Hill, D. J. T.; Killeen, M. I.; O'Donnell, J. H.; Pomery, P. J.; John, D. S.; Whittaker, A. K. J Appl Polym Sci 1996, 61, 1757.
13. Kayaman-Apohan, N.; Demirci, R.; Cakir, M.; Gungor, A. Radiat Phys Chem 2005, 73, 254.
14. Su, T.; Wang, G. Y.; Xu, X. D.; Hu, C. P. J Polym Sci Part A: Polym Chem 2006, 44, 3365.
15. Feng, L.; Zhang, X.; Dai, J.; Ge, Z.; Chao, J.; Bai, C. Front Chem China 2008, 3, 1.
16. Mohammad Rabea, A.; Mohseni, M.; Mirabedini, S. M. JCT Res 2011, 8, 497.
17. Ahadian, S.; Mohseni, M.; Moradian, S. Int J Adhes Adhes 2009, 29, 458.
18. Wu, W.; Nancollas, G. Adv Colloid Interface Sci 1999, 79, 229.
19. Owens, D. K.; Wendt, R. C. J Appl Polym Sci 1969, 13, 1741.
20. McLaren, K. J Soc Dyes Colour 1976, 92, 338.
21. Graiver, D.; Farminer, K. W.; Narayan, R. J Polym Environ 2003, 11, 129.
22. Kim, H.; Urban, M. W. Langmuir 2000, 16, 5382.
23. Jalili, M. M.; Moradian, S. Prog Org Coat 2009, 66, 359.
24. Wenzel, R. N. Ind Eng Chem 1936, 28, 988.